Original Article

Calcium-overloaded sympathetic preganglionic neurons in a case of severe sepsis with anorexia nervosa

Miyuki Kinebuchi and Akihiro Matsuura

Department of Molecular Pathology, Graduate School of Medicine, Fujita Health University, Toyoake, Aichi, Japan

Aim: We aimed to show the status of intracellular elements in sympathetic preganglionic neurons in an autopsy case of a 55-year-old woman with severe sepsis and cardiac dysfunction with anorexia nervosa.

Methods: Our methods include a case report and pathological examinations of autopsied tissues using synchrotron-generated microbeam X-ray fluorescence analysis.

Results: A case report of severe sepsis and myocardial dysfunction. The patient had sudden short cardiac arrest without arrhythmia and sequelae, and echocardiogram showed negative inotropic change. The X-ray fluorescence analysis of autopsied tissues indicated an unusually high concentration of cytosolic calcium in sympathetic preganglionic neurons. However, there were no significant pathological findings of damage in the heart or the cardiovascular autonomic nuclei in the central nervous system.

Conclusion: The data indicate that dysfunction of the sympathetic preganglionic neurons exists in a patient of severe sepsis and cardiac dysfunction with anorexia nervosa.

Key words: Anorexia nervosa, autonomic nervous system, cardiac arrest, central nervous system, circulation, cytosolic calcium, severe sepsis, sympathetic preganglionic neurons, synchrotron based pathological diagnosis

INTRODUCTION

Cardiac dysfunction contributes to the high mortality of sepsis.[1] It is a complex, multifactorial process. There are many septicemic inflammatory factors involved in negative inotropic change, resulting in cardiac dysfunction.[2] Furthermore, Toll-like receptor signals, through common myeloid differentiation factor 88 signaling and/or the Toll/interleukin-1 receptor domain-containing adaptor inducing interferon-β-mediated transcription factor signaling, involve cardiac injury.[3] However, many clinical trials against these mediators and receptors have not proven to alter mortality or outcome of severe sepsis.

Furthermore, several animal experiments of sepsis induced by gram-negative and/or gram-positive bacteria revealed that cardiomyocytes with decreased contractility showed decreased cardiac myofilament sensitivity to Ca^{2+} and reduced Ca^{2+}-transients.[4,5] The latter was caused by diminished L-type calcium channels and oxidized sarco(endo)plasmic Ca^{2+}-ATPase.[6] Although the β-adrenergic receptor agonist isoproterenol could reverse the calcium dynamics of septicemic cardiomyocytes in the experiment,[7] many severely septic patients do not respond to multiple vasopressors.

The autonomic nervous system (ANS) reflexively regulates the inflammatory response in real time.[8] Activation of efferent vagus nerve decreases proinflammatory cytokine levels in liver, spleen, heart, and macrophages.[8] Activation of efferent sympathetic nerve can increase local catecholamine level to suppress inflammation.[8] Furthermore, stimulation of afferent vagus nerve stimulates the hypothalamic–pituitary–adrenal axis, that is, the humoral anti-inflammatory pathway by glucocorticoids.[8]

Dysregulation of ANS exists in sepsis,[2] and is supposed to be crucial to cure patients with severe sepsis. However, detailed status of the sympathetic nervous system regulating blood pressure and cardiac function in sepsis has not been well characterized. For example, lipopolysaccharides increase the plasma norepinephrine level that is secreted from adrenal chromaffin cells.[9] When norepinephrine increases over a long term, like congenital heart failure, it becomes toxic for cardiac sympathetic nerve terminals.[10] Lipopolysaccharides suppress postsynaptic sympathetic nerve activity to

Corresponding: Miyuki Kinebuchi, MD, Department of Molecular Pathology, Graduate School of Medicine, Fujita Health University 1-98, Dengakugakubo, Toyoake, Aichi 470-1192, Japan. E-mail: mkine@fujita-hu.ac.jp.
Received 7 Jun, 2014; accepted 19 Oct, 2014; online publication 15 December, 2014

the muscle vascular bed, but do not result in hypotension in healthy humans.[11] Furthermore, dysregulation of ANS activity by N-type Ca^{2+} channels can trigger ventricular arrhythmias and sudden death in the mouse model.[12] Here we reveal the intracellular calcium status of sympathetic preganglionic neurons (SPN) using a synchrotron-generated microbeam X-ray fluorescence (XRF) analysis in an autopsied patient with severe sepsis and AN.

METHODS

Case report

THIS STUDY WAS approved by the institutional ethics committee of the Fujita Health University (Ethical Review Board for Epidemiological and Clinical Studies: registration number 06-051, 09-064) and followed ethical guidelines. Informed consent was obtained from the patient's family member because the patient had died. The key data were detected using a synchrotron. Synchrotron radiation-based XRF analysis has been established over the past 30 years to detect elements in materials.[13] We show here our method of a synchrotron-generated microbeam XRF analysis, which has been published as a SPring-8 user report.[14]

Sample preparation

The specimens obtained by autopsy were processed to the formalin-fixed paraffin-embedded tissue sections with 2-μm thickness and placed on to Kapton film (10-μm thickness; Teijin DuPont, Tokyo, Japan). After removal of paraffin with xylene and rehydration with ethanol, these sections were stained with hematoxylin–eosin for histological examination.

Synchrotron radiation experiments

The BL37XU beamline in the SPring-8, a third-generation synchrotron radiation facility (JASRI, Hyogo, Japan) is for trace element analysis. The beam was focused to a spot size of 0.5–1.1 μm (vertical) × 0.9–1.5 μm (horizontal) with a measured flux of more than 10^{11} photons/s at 10 keV using Pt-coated Kirkpatrick–Baez focusing optics at a glancing angle of 2.8 mrad. A processed sample was mounted on the XY-scanning stage at a takeoff angle of 10°, and X-ray fluorescence was detected with an energy-dispersive X-ray detector (single-element silicon drift detector; Roentec, Berlin, Germany) oriented perpendicular to the incident beam. The resultant fluorescence X-ray emission was analyzed with energy dispersive spectrometry. The fluorescence counts were extracted from energy dispersive spectra by setting regions about the respective X-ray emission lines (Ca Kα; 3.7 keV, Cu Kα; 8.0 keV, and Zn Kα; 8.6 keV). The pixel size 2.5 μm × 2.5 μm was used to distinguish the observation objects at the subcellular level, and the detection area of 220 μm^2 was used for experiments. The data were collected for 0.5 s/pixel. The datasets from each pixel were calculated. The photon count quantity was expressed according to a scale of the rainbow color, and a 2D map was constructed using LabView (National Instruments Japan, Tokyo, Japan) and IGOR pro (WaveMetrics, Lake Oswego, OR, USA).

Quantification of element in thin tissue sections

The biochemical Ca contents and the averaged fluorescence yields (photon counts obtained by single-element silicon drift detector) of the formalin-fixed paraffin-embedded tissue sections were plotted on a scatter diagram. To compare results of different beamtimes, the fluorescence X-ray intensity was normalized by the incident beam intensity. The fluorescence yields (I_f; photon counts) in each pixel was divided by I_0 (incident X-ray) in the same pixel.

RESULTS

A 57-YEAR-OLD WOMAN PRESENTED to our hospital with a 2-day history of fever and a 1-day history of abdominal and back pain, and difficulty with breathing. She had been diagnosed with anorexia nervosa (AN) (height, 150 cm; weight, 21.5 kg; body mass index [BMI], 9.6) at 55 years of age. At that time she was suffering from right radial nerve palsy, and was treated first for malnutrition. Then she developed refeeding syndrome, and electrolyte and fluid imbalances were corrected. In addition, she was diagnosed with primary hypothyroidism and began taking levothyroxine sodium hydrate. There were no abnormalities in cardiac function or other endocrine systems. She was then treated as an outpatient with AN (BMI 10~12), primary hypothyroidism, and mild renal dysfunction. Throughout the course of her treatment, the following symptoms were not observed in the patient: desire to lose weight; fear of weight gain; and abnormal eating behavior, besides an aversion to eating rice. The patient's BMI was extremely low but stable. She was relatively well, underwent nutritional guidance and a blood chemistry test once a month, and was supplemented with oral prosultiamine (100 mg/day).

On admission, she was alert and conscious with peripheral coldness, hypotension, tachycardia, and fever. Blood analysis and radiograph revealed sepsis with pneumonia and extensive gas formation in the large intestine (Table 1). On day 1, despite treatment with i.v. fluid therapy, vasopressor

Table 1. Time course of physical examination and laboratory data of a 55-year-old woman with severe sepsis and cardiac dysfunction with anorexia nervosa

	On admission	Day 2	Day 3
Body temperature, °C	37.9	37.9	34.6
Heart rate, b.p.m.	134	126	110
Pupil size, mm	Normal	Normal	R = 6, L = 4
Pupillary light reflex	Normal	Normal	Poor
Blood pressure, mmHg	78/45	Not detected	74/39
CVP, mmHg	ND	5	8.6
WBC, cells/mm^3	1,500	3,600	3.200
RBC, $\times 10^6$ per mm^3	4.85	3.08	2.70
Hb, g/dL	14.5	9.0	7.7
Ht, %	43.7	26.8	23.7
Plat, $\times 10^3$ per mm^3	140	1.2	2.0
CPK-MB (EIA), IU/L	ND	41.7	ND
Blood glucose level, mg/dL	49	231	124
Cardiac troponin I, ng/mL	ND	0.07	ND
Total protein, g/dL	5.8	3.6	4.1
Albumin, g/dL	2.4	2.1	2.4
CRP, mg/dL	38.6	12.0	9.1
T. Bil, mg/dL	0.9	1.2	2.3
D. Bil, mg/dL	ND	0.8	1.5
GOT, IU/L	92	143	269
GPT, IU/L	32	41	74
LDH, IU/L	ND	268	557
ALP, IU/L	ND	409	611
γ-GTP, IU/L	ND	39	45
LAP, IU/L	ND	61	84
ChE, IU/L	ND	15	69
Amylase, IU/L	162	431	282
CPK, IU/L	195	735	2,359
Neutral fat, mg/dL	ND	130	ND
Total cholesterol, mg/dL	ND	40	ND
BUN, mg/dL	111.5	85.0	27.4
Uric acid, mg/dL	ND	3.7	1.1
Creatinine, 1.33 mg/dL	1.33	1.28	0.42
Serum Na, mEq/L	126	128	136
Serum K, mEq/L	4.5	4.3	3.3
Serum Cl, mEq/L	90	101	104
Serum Ca, mg/dL	8.3	5.8	8.3
Serum P, inorganic, mg/dL	ND	6.4	2.9
PH	7.363	7.110	7.161
$PaCO_2$	33.4	41.3	53.5
PaO_2	49.6	167.9	54.9
HCO_3	18.6	12.8	18.7
BE	–5.8	–15.7	–9.5
O_2SAT	84.2	98.5	87.0
PT (INR)	1.26	1.52	1.60
APTT, s	25.0	42.3	115.4
FDP, μg/mL	10.4	12.4	16.1
D-dimer (LPIA), μg/mL	3.8	4.9	5.4
Antithrombin III, %	48	43	74

ALP, akaline phosphatase; APTT, activated partial thromboplastin time; BE, base excess; BUN, blood urea nitrogen; ChE, cholinesterase; CPK-MB, creatine phosphokinase brain and muscle type; CRP, C-reactive protein; CVP, central venous pressure; D. Bil, direct bilirubin; EIA, enzyme immuno assay; FDP, fibrin/fibrinogen degradation products; GOT, glutamic oxaloa cetic transaminase; GPT, glutamic pyruvic transaminase; γ-GTP, γ-gluta myltransferase; Hb, hemoglobin; Ht, hematocrit; L, left; LAP, leucine am inopeptidase; LDH, lactate dehydrogenase; LPIA, latex coagulating method; O2SAT, oxygen saturation; PH, potential hydrogen; Plat, platelet count; PT (INR), prothrombin time international normalized ratio; R, right; RBC, red blood cell count; T. Bil, total bilirubin; WBC, white blood cell count.

agents (0.45 μg/kg/min norepinephrine infusion), wide-spectrum antibiotics (1.5 g/day meropenem i.v.), γ-globulin (6 g/day i.v.), and mechanical ventilatory support with a propofol infusion (1.3 mg/kg/h), she developed severe hypotension. On day 2, blood cultures confirmed the presence of *Escherichia coli*, *Streptococcus pneumoniae*, and *Streptococcus bovis*. During endotoxin adsorption therapy using Toraymyxin (Toray Medical Co., Ltd., Tokyo, Japan) and a continuous hemodiafiltration (volume of blood flow 120 mL/min) with nafamostat mesilate (1 mg/kg/h) and ulinastatin (100,000 IU/day), the patient developed cardiac arrest without arrhythmia or other causes, and recovered after immediate treatment without sequelae. Echocardiography showed a diffuse reduction in contractile capacity and a decreased left ventricular ejection fraction (30%). Despite additional dopamine hydrochloride (3 μg/kg/min), dobutamine hydrochloride (3 μg/kg/min), and gabexate mesilate (30 mg/kg/day) infusions, she developed hypothermia, metabolic acidosis, and disseminated intravascular coagulation (Table 1). Serum K (4.5 mEq/L) and serum P inorganic (6.4 mg/dL) were within normal ranges, contradictory to the diagnosis of refeeding syndrome. On day 3, the patient's pupils completely dilated with a loss of reflex to light and loss of doll's head eye phenomenon, followed by cardiac arrest and death.

Table 2. Pathological findings of disseminated intravascular coagulation in an autopsy case of a 55-year-old woman with severe sepsis and cardiac dysfunction with anorexia nervosa

Fibrinous microthrombi	Several glomerular capillaries
	Capillaries of frontal cortex in the watershed territory
Microhemorrhage	Gastric mucosa
	Endometrium
	Ovary
	Pancreas
	Gray matter of spinal cord

Autopsy findings were acute bilateral lobar pneumonia with pleuritis and pleural effusion, fibrinous pericarditis, atrophic thyroid without inflammation, contracted kidney with focal segmental glomerulonephritis, septicemic splenitis, septicemic colitis (neutrophil infiltration in the submucosal layer of the intestine, colon, and upper part of the rectum), and disseminated intravascular coagulation (Table 2). The central nervous system (CNS) including autonomic nuclei appeared to be intact, except for fibrinous microthrombi in the capillaries of the frontal cortex in watershed territory. Unexpectedly, the calcium concentration in SPNs in the lateral horn of spinal cord T1 was remarkably increased, detected by a synchrotron-generated XRF analysis (Fig. 1). The other elemental contents, such as zinc and copper, were not unusual.

We concluded that the patient's condition progressed from pneumonia to sepsis, then to septic shock. During treatment the patient did not respond to any vasopressor agents and presented with sudden short cardiac arrest without arrhythmia or sequelae. Echocardiogram showed negative inotropic change, which corresponds to septicemic cardiomyopathy. Autopsy revealed an unusually high concentration of cytosolic calcium in SPNs; these cells did not show any apoptotic findings by chromatin condensation or cell shrinkage. There were no significant pathological findings of damage in the heart or cardiovascular autonomic nuclei in the CNS of this patient.

DISCUSSION

SEPSIS STARTS WITH arterial hypotension and variable organ dysfunction, subsequently accompanied with refractory hypotension and multiple organ failure. Kidney, heart, brain, and liver are often damaged organs. Neuronal death in cardiovascular autonomic nuclei in the CNS was previously reported in patients with septic shock, which was suggested to correlate with vascular iNOS expression.[15,16] Ours was clearly a case of sepsis with refractory hypotension and cardiac dysfunction. The patient's heart and brain areas regulating cardiovascular function did not show any

Fig. 1. Elemental content of the spinal cord T1 in an autopsy case of a 55-year-old woman with severe sepsis and cardiac dysfunction with anorexia nervosa. A, Spinal cord T1 level of the patient stained with Luxol fast blue and hematoxylin–eosin. Luxol fast blue dyes myelin sheath blue. The area analyzed by X-ray fluorescence (XRF) is surrounded by a black line. B, Photograph showing the area analyzed by XRF, using a stereoscopic microscope. C–E, XRF analysis using the beamline BL37XU at SPring-8. Each element was detected using specific X-ray energy (Kα). Calcium, copper, and zinc are detected at Kα 3.7 KeV, Kα 8 KeV, and Kα 8.6 KeV, respectively. Detected photon counts (*z*) in a particular X-ray energy at a location (*x*, *y*) are expressed according to a scale of the rainbow color (right bar). F, Spinal cord T1 level of a patient with cardiogenic shock due to cardiomyopathy, showing analyzed area using stereoscopic microscopy. C, G, Zinc at Kα 8.6 KeV. D, H, Calcium at Kα 3.7 KeV. E, I, Copper at Kα 8 KeV.

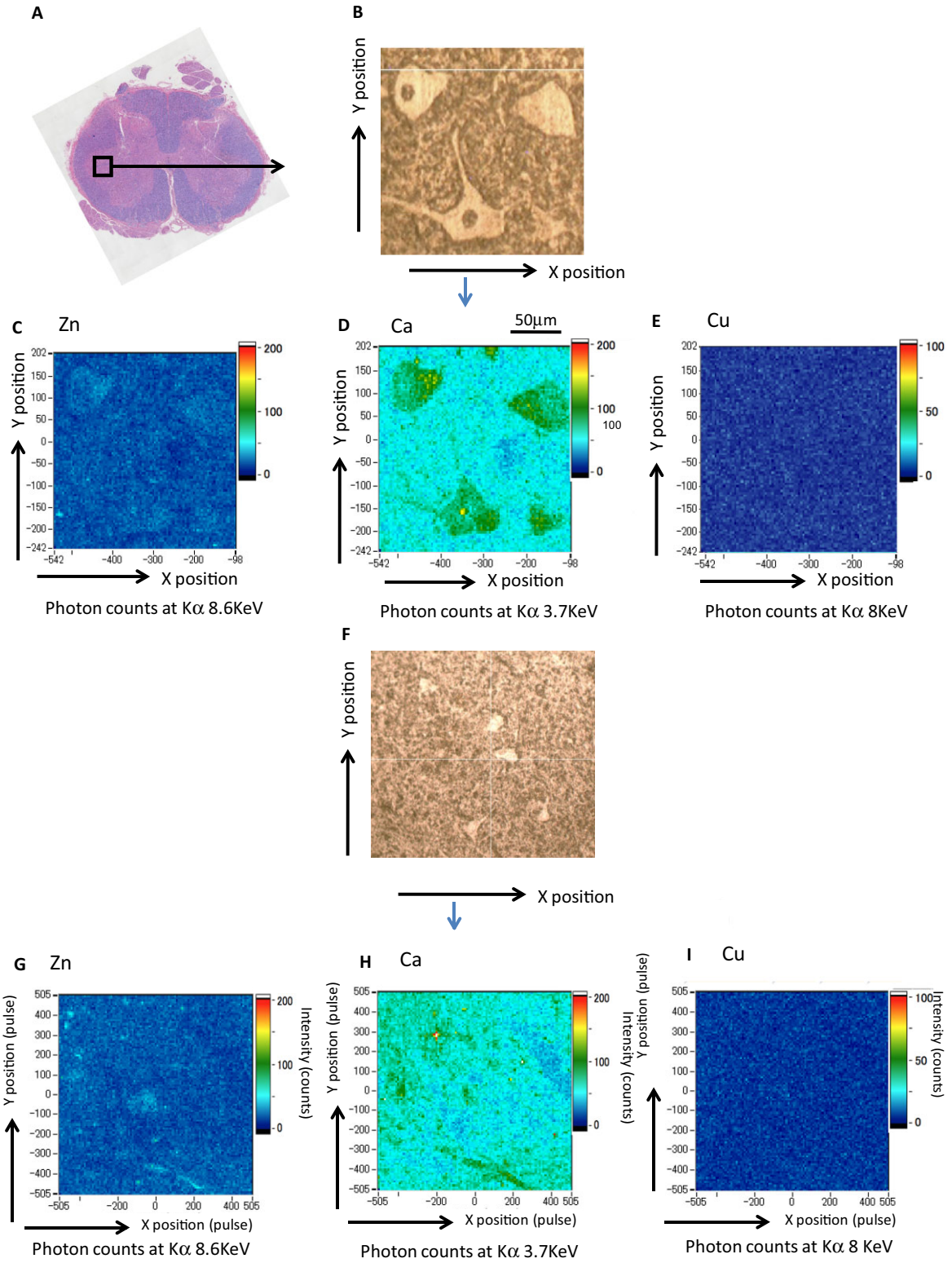

pathological findings. We then analyzed SPNs that originated from the lateral horn of spinal cord using synchrotron-based XRF analysis, which can specifically detect an element. Unusually, the shape of the cell bodies of SPN was visualized clearly by highly increased intracellular calcium ([Ca]i) (Fig. 1A–G). As a control example, Figure 1(F–I) shows another SPN in a patient with cardiogenic shock due to cardiomyopathy. In the control case, [Ca]i of the SPN was not increased. The patient's increased [Ca]i of SPN suggested the disruption of neuronal calcium homeostasis. In general, Ca^{2+} enters neuronal cytosol through voltage-gated Ca^{2+} channels, *N*-methyl-*D*-aspartate receptors, α-amino-3-hydroxy-5-methyl-4-isoxazolepropionic acid receptors, and store-operated channels on the plasma membrane.[17] Furthermore, Ca^{2+} release from endoplasmic reticulum (ER) to cytosol through inositol 1,4,5-triphosphate receptors, ryanodine receptors, and presenilins.[16] In contrast, Ca^{2+} release from neuronal cytosol to extracellular through the plasma membrane Ca^{2+} ATPases and sodium/calcium exchangers, and to ER through sarco(endo)plasmic Ca^{2+}-ATPase.[16] Mitochondrial calcium homeostasis has not been fully elucidated. It has been reported that Ca^{2+} enters mitochondria through voltage-dependent anion channels and the mitochondrial uniporter.[16] If mitochondrial permeability transitional pores open, large amounts of Ca^{2+} are released from mitochondria to cytosol.[17] Previously, it was shown that dysregulation of calcium homeostasis led to neuronal cell death from dysfunction in aging neurons, and the damaged neurons of the Alzheimer's disease and amyotrophic lateral sclerosis have been observed.[17,18] Vitamin B1 deficiency leads to oxidative stress in animals and human cultured cells.[19] This patient had been taking vitamin B complex for 2 years, since being diagnosed with, and treated for, AN. Beriberi heart, caused by lack of vitamin B1, results in high-output heart failure, but she had no evidence of this deficiency. Although her cardiac function was normal until the last admission, there is a possibility that her heart function reserve was reduced, for example, due to persisting AN. In patients with AN, several groups have reported that parasympathetic/sympathetic imbalance exists; there is a shift in cardiac autonomic function toward parasympathetic predominance,[20] and adrenal sympathetic over-activity with neural sympathetic underactivity.[21]

In fact, elevated [Ca]i in SPN was observed in this patient. It was reported that both oxidative stress and tumor necrosis factor (TNF) stimulate ryanodine receptor on the membrane of ER to release Ca^{2+} from ER to the cytoplasm of neurons.[22,23] We speculated that inflammatory cytokines and oxidative stress caused by sepsis result in acutely increased [Ca]i of the SPN cell body, and subsequently lead to neuronal dysfunction. Furthermore, a signal from G-protein-coupled receptors on the plasma membrane can stimulate inositol 1,4,5-triphosphate receptors on ER to release Ca^{2+} from ER to the cytoplasm of neurons.

CONFLICT OF INTEREST

NONE.

ACKNOWLEDGEMENTS

WE WOULD LIKE to thank Shinohara Kunio, Ninomiya Toshio, and Komiya Satoshi for discussions about the initiation of this study in 2005 at SPring8. We also thank Terada Yasuko for excellent technical assistance at SPring8. The study was supported by the Japan Society for the Promotion of Science Kakenhi Grants-in-Aid 24659503 and 26461534 to Akihiro Matsuura and Miyuki Kinebuchi, and the Japan Synchrotron Radiation Research Institute (No. 2006A1809, 2006B1712, 2007A1852, 2007B1724, 2008A1659, 2008A1871, 2008B1825, 2008B1986, 2009A1704, 2009B1723, 2009B1925, 2010A1327, 2010B1700, 2011A1633, 2011B1715).

REFERENCES

1 Dellinger RP, Levy MM, Rhodes A *et al.*; Surviving Sepsis Campaign Guidelines Committee including the Pediatric Subgroup. Surviving sepsis campaign: International guidelines for management of severe sepsis and septic shock, 2012. Crit. Care Med. 2013; 41: 580–637.

2 Antonucci E, Ficcadori E, Donadello K, Taccone FS, Franchi F, Scolletta S. Myocardial depression in sepsis: From pathogenesis to clinical manifestations and treatment. J. Crit. Care 2014; 29: 500–11.

3 Feng Y, Zou L, Zhang M, Li Y, Chen C, Chao W. MyD88 and Trif signaling play distinct roles in cardiac dysfunction and mortality during endotoxin shock and polymicrobial sepsis. Anesthesiology 2011; 115: 555–67.

4 Sips PY, Irie T, Zou L *et al.* Reduction of cardiomyocyte S-nitrosylation by S-nitrosoglutathione reductase protects against sepsis-induced myocardial depression. Am. J. Physiol. Heart Circ. Physiol. 2013; 304: H1134–46.

5 Zhong J, Hwang TC, Adams HR, Rubin LJ. Reduced L-type calcium current in ventricular myocytes from endotoxemic guinea pigs. Am. J. Physiol. Heart Circ. Physiol. 1997; 273: H2312–24.

6 Hobai IA, Buys ES, Morse JC *et al.* SERCA Cys^{674} sulphonylation and inhibition of L-type Ca^{2+} influx contribute to cardiac dysfunction in endotoxemic mice, independent of cGMP synthesis. Am. J. Physiol. Heart Circ. Physiol. 2013; 305: H1189–200.

7 Abi-Gerges N, Tavernier B, Mebazaa A *et al*. Sequential changes in autonomic regulation of cardiac myocytes after *in vivo* endotoxin injection in rat. Am. J. Respir. Crit. Care Med. 1999; 160: 1196–204.
8 Tracey KJ. The inflammatory reflex. Nature 2002; 420: 853–9.
9 Lukewich MK, Lomax AE. Endotoxemia enhances catecholamine secretion from male mouse adrenal chromaffin cells through an increase in Ca^{2+} release from the endoplasmic reticulum. Endocrinology 2014; 155: 180–92.
10 Liang C, Rounds NK, Dong E, Stevens SY, Shite J, Qin F. Alterations by norepinephrine of cardiac sympathetic nerve terminal function and myocardial β-adrenergic receptor sensitivity in the ferret. Circulation 2000; 102: 96–103.
11 Sayk F, Vietheer A, Schaaf B *et al*. Endotoxin causes central downregulation of sympathetic vasomotor tone in healthy humans. Am. J. Physiol. Regul. Integr. Comp. Physiol. 2008; 295: R891–8.
12 Yamada Y, Kinoshita H, Kuwahara K *et al*. Inhibition of N-type Ca^{2+} channels ameliorates and imbalance in cardiac autonomic nerve activity and prevents lethal arrhythmias in mice with heart failure. Cardiovasc. Res. 2014; 104: 183–93. doi: 10.1093 [ahead of print].
13 Paunesku T, Vogt S, Maser J, Lai B, Woloschak G. X-ray fluorescence microprobe imaging in biology and medicine. J. Cell. Biochem. 2006; 99: 1489–502.
14 Matsuura A, Kinebuchi M, Terada Y. Histopathologic basis of neuronal tissues by microbeam XRF (X-ray fluorescence analysis). Result report of medical bio EX proposal. 2009; 2009B: 170–1 [cited 31 March 2010]. Available from: http://www.spring8.or.jp/pdf/ja/MBTU/H21/18.pdf.
15 Sharshar T, Gray F, de la Grandmaison G *et al*. Apoptosis of neurons in cardiovascular autonomic centres triggered by inducible nitric oxide synthase after death from septic shock. Lancet 2003; 362: 1799–805.
16 Sharshar T, Annane D, de la Grandmaison GL, Brouland JP, Hopkinson NS, Françoise G. The neuropathology of septic shock. Brain Pathol. 2004; 14: 21–33.
17 Supnet C, Bezprozvanny I. Neuronal calcium signaling, mitochondrial dysfunction, and Alzheimer's disease. J. Alzheimers Dis. 2010; 20: S487–98.
18 Tadic V, Prell T, Lautenschlaeger J, Grosskreutz J. The ER mitochondria calcium cycle and ER stress response as therapeutic targets in amyotrophic lateral sclerosis. Front. Cell. Neurosci. 2014; 8: 147. doi: 10.3389/fncel.2014.00147.
19 Huang HM, Chen HL, Gibson GE. Thiamine and oxidants interact to modify cellular calcium stores. Neurochem. Res. 2010; 35: 2107–16.
20 Clancy JA, Mary DA, Witte KK, Greenwood JP, Deuchars SA, Deuchars J. Non-invasive vagus nerve stimulation in healthy humans reduces sympathetic nerve activity. Brain Stimul. 2014; pii: S1935-861X(14)00260-5. doi: 10.1016/j.brs.2014.07.031.
21 Lechin F, van der Dijs B, Pardey-Maldonado B, Rivera JE, Baez S, Lechin ME. Anorexia nervosa depends on adrenal sympathetic hyperactivity: Opposite neuroautonomic profile of hyper insulinism syndrome. Diabetes Metab. Syndr. Obes. 2010; 3: 311–7.
22 Anzai K, Ogawa K, Kuniyasu A, Ozawa T, Yamamoto H, Nakayama H. Effects of hydroxyl radical and sulfhydryl reagents on the open probability of the purified cardiac ryanodine receptor channel incorporated of the purified cardiac ryanodine receptor channel incorporated into planar lipid bilayers. Biochem. Biophys. Res. Commun. 1998; 249: 938–42.
23 Rogers RC, van Meter MJ, Hermann GE. Tumor necrosis factor potentiates central vagal afferent signaling by modulating ryanodine channels. J. Neurosci. 2006; 26: 12642–6.